Available online at www.sciencedirect.com
ScienceDirect
Journal of Photochemistry and Photobiology A: Chemistry 184 (2006) 241–249
Journal of Photochemistry and Photobiology A:Chemistry
www.elsevier.com/locate/jphotochem

Synthesis and DNA binding studies by spectroscopic and PARAFAC methods of a ternary copper(II) complex

Fang Zhang [a], Qian-qian Zhang [a,*], Wei-guo Wang [b], Xiu-lin Wang [a]

[a] College of Chemistry and Chemical Engineering, Ocean University Of China, Qingdao 266003, PR China
[b] Department of Mathematics, Ocean University Of China, Qingdao 266071, PR China

Received 15 December 2005; received in revised form 22 March 2006; accepted 22 April 2006
Available online 21 June 2006

Abstract

A new ternary copper(II) complex, $[Cu_2(DL\text{-}Asp)(phen)_3]SO_4{\cdot}4H_2O$ (Phen = 1,10-phenanthroline, DL-Asp = DL-aspartic acid), has been synthesized and characterized by element analysis, infrared spectra and thermal analysis. Spectroscopic studies, including electronic absorption and fluorescence spectra, and parallel factor analysis (PARAFAC) of fluorescence excitation-emission three-way data array were carried out on the DNA binding modes of the complex. The results suggest that at low molar ratio of the complex to DNA (0.25 at most), the end of four-coordinated Cu(II) of the complex binds to DNA by hydrogen bond, which induces the breakage of the secondary structure of DNA. Otherwise, the six-coordinated Cu(II) end of the complex intercalates into the base pair of DNA. Electrostatic effect also takes place between the complex cation and the phosphate group of DNA. Additionally, the equilibrium concentrations of EB-DNA and EB (EB = ethidium bromide) could be directly obtained by PARAFAC algorithm. The results of PARAFAC also indicate that, the conformation of the DNA is changed from B form to BZ mixed form by the interaction with the complex; EB may interact with BZ-DNA by cooperative binding which has a higher affinity than by intercalation with B-DNA. The PARAFAC algorithm is proved a convincing method for studying the interaction of complexes with DNA.

Keywords: Ternary copper(II) complex; Synthesis; DNA binding; PARAFAC algorithm

1. Introduction

Copper has been recognized as an essential trace metal for living organisms since the late 1930s [1]. 1,10-Phenanthroline is one of the earliest and most extensively studied N-heterocyclic chelating agents. Because of the potential application as nonradioactive nucleic acid probes and DNA cleaving agents, the complexes of 1,10-phenanthroline and other polypyridyls with transition metals have stimulated various researches [2]. Thus, the copper(II) complexes of 1,10-phenanthroline and its derivatives and some ternary copper(II) complexes containing them, attract great attentions since they exhibit numerous biological activities such as antitumor, anti-Candida, antimycobacterial, and antimicrobial activity, etc. [2–9]. Moreover, considerable attention has been focused on the use of phenanthroline complexes as intercalating agents of DNA [10] and as artificial nucleases [9–13]. Amino acids are the basic structural units of proteins. Copper complexes of amino acids and 1,10-phenanthroline were reported to exhibit potent antitumor and artificial nuclease activity [9,14].

In this paper, a ternary copper(II) complex, $[Cu_2(DL\text{-}Asp)(phen)_3]SO_4{\cdot}4H_2O$ (Phen = 1,10-phenanthroline, DL-Asp = DL-aspartic acid) has been synthesized and characterized. The two central copper atoms in the complex are of different coordination patterns (Fig. 1). Both the traditional spectroscopic methods (electronic absorption spectra and fluorescence spectra) and parallel factor analysis (PARAFAC) were utilized to carry out the DNA binding studies. The introduction of the PARAFAC is as follows:

1.1. Trilinear model

A PARAFAC model of a three-way array is given by three loading matrices A, B and C with elements a_n, b_n and c_n. If K equilibrious mixtures containing N fluorescing components were measured at I excitation and J emission wavelengths, the K of $I \times J$ matrices of the excitation-emission fluorescence

* Corresponding author. Tel.: +86 532 82032481; fax: +86 532 82032483.
E-mail address: qqzhang@ouc.edu.cn (Q.-q. Zhang).

1010-6030/$ – see front matter © 2006 Elsevier B.V. All rights reserved.
doi:10.1016/j.jphotochem.2006.04.028

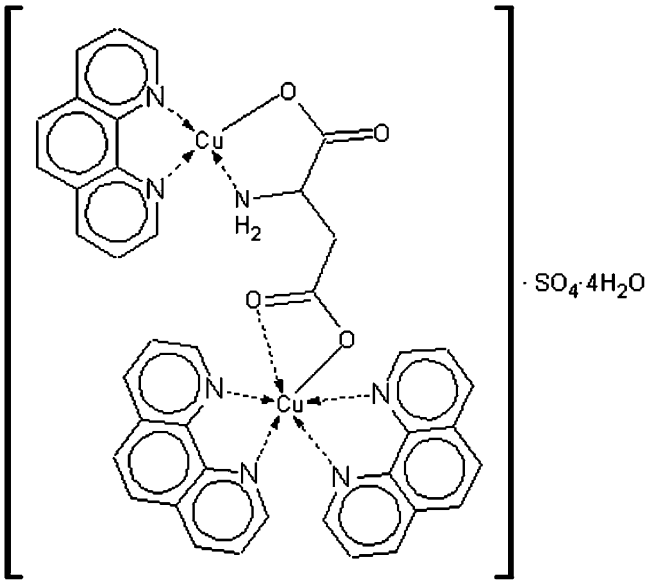

Fig. 1. The structure of $[Cu_2(DL\text{-}Asp)(phen)_3]SO_4{\cdot}4H_2O$.

spectra could be obtained. An $(I \times J \times K)$ three-way data array X is formulated by the K of $(I \times J)$ matrices as follows [15]:

$$X_{I\times J\times K} = \sum_{n=1}^{N} a_n \otimes b_n \otimes c_n + E_{I\times J\times K}$$

Here the symbol $\otimes$ denotes a tensor product; a_n, b_n and c_n are excitation, emission and concentration profiles of the nth fluorescing chemical component, respectively; E is a three-way array of residuals.

The trilinear model can also be expressed as follows:

$$X_{\ldots K} = A\,\mathrm{diag}(c_{(k)})B^{\mathrm{T}} + E_{\ldots k} \quad (k = 1, 2, \ldots, K)$$

In the above equation, $X_{\ldots K}$ and $E_{\ldots K}$ are the kth matrix slices of X and E along the K-mode; the superscript 'T' denotes transpose of a matrix; $\mathrm{diag}(c_{(k)})$ denotes the diagonal matrix whose diagonal elements are the corresponding ones of the kth row vector $c_{(k)}$ of the concentration matrix $C_{K\times N}$.

1.2. Algorithm of PARAFAC

By alternating least squares (ALS) by successively assuming the loadings in two modes known and then estimating the unknown set of parameters of the last mode, we can find the solution to the PARAFAC model [16].

The three-way arrays are unfolded to matrices. The $I \times JK$ matrix is termed $X^{(1)}$, where the superscript indicates that it is the first mode that is preserved. Likewise, $X^{(2)}$ is a $J \times IK$ matrix and $X^{(3)}$ is a $K \times IJ$ matrix. The PARAFAC model can be expressed for the matrix array $X^{(1)}$:

$$X^{(1)} = A(C| \otimes |B)^{\mathrm{T}} + E^{(1)}$$

where the sign $|\otimes|$ stands for the Khatri–Rao product [17]. A is determined easily by least squares, if the estimates of B and C are known. If $Z = (C|\otimes|B)^{\mathrm{T}}$, then A is defined as:

$$X^{(1)} = AZ$$

The least squares estimate of A is $A = X^{(1)}\,Z^{+}$, where Z^{+} is the Moore–Penrose inverse of Z. If Z has the row full rank, then the Moore–Penrose inverse can be written as $Z^{+} = Z^{\mathrm{T}}\,(ZZ^{\mathrm{T}})^{-1}$. Therefore, the conditional least squares estimate of C is

$$A = X^{(1)}Z^{\mathrm{T}}(ZZ^{\mathrm{T}})^{-1}$$

Likewise, B and C can be obtained.

The general PARAFAC ALS algorithm can be written as follows:

(1) Estimate the number of components N;
(2) Initialize A and B;
(3) Estimate C from X, A and B by least squares:

$$c_{(k)} = \mathrm{diag}(A^{\mathrm{T}}X_{\ldots k}B)^{\mathrm{T}}[(A^{\mathrm{T}}A) * (B^{\mathrm{T}}B)]^{-1}$$
$$(k = 1, 2, \ldots, K)$$

where $C_{(k)}$ is the kth row vector of matrix C; symbol '*' denotes a Hadamard product [17]. That is, if $C_{M\times N} = A_{M\times N} * B_{M\times N}$ for $(M \times N)$ matrices A, B, C, then $c_{mn} = a_{mn} \times b_{mn}$, where c_{mn}, a_{mn} and b_{mn} are elements of the mth row and nth column of matrices C, A, and B, respectively.

(4) Estimate A from X, C and B:

$$A = \left[\sum_{k=1}^{K} X_{\ldots k}B\,\mathrm{diag}(c_{(k)})\right]\left[\sum_{k=1}^{K}\mathrm{diag}(c_{(k)})BB^{\mathrm{T}}\,\mathrm{diag}(c_{(k)})\right]^{-1}$$

(5) Estimate B from X, A and C:

$$B = \left[\sum_{k=1}^{K} X^{\mathrm{T}}_{\ldots k}A\,\mathrm{diag}(c_{(k)})\right]\left[\sum_{k=1}^{K}\mathrm{diag}(c_{(k)})AA^{\mathrm{T}}\mathrm{diag}(c_{(k)})\right]^{-1}$$

(6) Return to step (3), until convergence.

2. Experimental

2.1. Apparatus

Elemental analyses for C, H and N were performed on a Perkin–Elmer240C analyzer. IR spectra were obtained on a Nicolet-ATAR360 spectrophotometer in the range of 4000–400 cm^{-1} as KBr pellets. The thermo analytical curves were obtained on a ZRY-2P Thermal Analyst, in static air, using α-alumina powder as standard with a heating rate of 10 °C min^{-1}. Electronic absorption spectra of DNA binding studies were recorded on a Shimadzu UV-2550 spectrophotometer. All the fluorescence spectra were recorded by a Hitachi F4500 fluorescence spectrophotometer. The three-dimension (3D) fluorescence spectra were recorded with the slit widths of 5 nm, scan wavelength intervals of 5 nm and a scan wavelength speed of 12000 nm/min. The ranges of excitation and emission wavelengths for all samples were 410–590 nm and 550–710 nm, respectively. The background was subtracted by using a reagent blank. The PARAFAC program compiled in MATLAB was used

to resolve the spectra and concentrations of EB-DNA and EB in equilibrious mixtures.

2.2. Materials

1,10-Phenanthroline monohydrate and DL-aspartic acid were both purchased from Shanghai, China. Fs DNA (fish sperm DNA) was purchased from Sigma, America. EB (ethidium bromide) was purchased from Amresco, America. All the materials were used as purchased and no further purification was carried out. At 260 and 280 nm, the absorbance ratio of solution fs DNA in Tris–NaCl buffer solution (50 mM Tris–HCl and 5 mM NaCl mixture, pH 7.0) equaled to 1.87:1, which indicated that the DNA was sufficiently free of protein [18]. The DNA concentration per nucleotide was determined by absorption spectra using the molar absorption coefficient ($6600\,M^{-1}\,cm^{-1}$) at 260 nm [19]; its stock solution was 5.15×10^{-3} M. The EB concentration was determined by absorption spectra using the molar absorption coefficient ($5680\,M^{-1}\,cm^{-1}$) at 480 nm [20]; its stock solution was 1.12×10^{-2} M. The complex Cu_2(DL-Asp)(phen)$_3$]$SO_4 \cdot 4H_2O$ was synthesized as bellow; its stock solution was 2.55×10^{-4} M. All the stock solutions were prepared by Milli-Q water and stored at 4 °C.

2.3. Preparation of [Cu_2(DL-Asp)(phen)$_3$]$SO_4 \cdot 4H_2O$

1,10-Phenanthroline monohydrate (1 mmol, 0.1982 g) was dissolved in 4 ml absolute ethanol; 10 ml aqueous solution of DL-aspartic acid (2 mmol, 0.2663 g) was added to the ethanol solution stirring at 60 °C; then 6 ml aqueous solution of cupric acetate monohydrate (1 mmol, 0.1995 g) was added to the mixture with continuous stirring. The pH of the mixture was adjusted to 3 with 2.0 M H_2SO_4. The hot mixture was filtered after being stirred for 7 h at 70 °C. The precipitate was washed several times with water and absolute ethanol, and then dried in a desiccator for 3 days. Then a kind of sky-blue powder was obtained. Analysis: calculated for $C_{40}H_{29}N_7O_8SCu_2 \cdot 4H_2O$ (%): C 49.69; H 3.83; N 10.14; found (%): C 49.40; H 3.90; N 10.35. IR (KBr pellet, cm^{-1}): 3478–3380m, 3221–3078s, 2950–2880m, 1650–1575vs, 1521s, 1429s, 1402vs, 1300m, 1101m, 1043m, 899w, 850s, 726s, 688 ~ 648w, 563m, 519w, 440m, cm^{-1} (vs, very strong; s, strong; m, medium; w, weak).

2.4. Procedure

2.4.1. Spectroscopic studies of [Cu_2(DL-Asp)(phen)$_3$]$SO_4 \cdot 4H_2O$ binding with DNA

Electronic absorption spectra of fs DNA (or [Cu_2(DL-Asp)(phen)$_3$]$SO_4 \cdot 4H_2O$) were recorded in the absence and presence of increasing amount of complex [Cu_2(DL-Asp)(phen)$_3$]$SO_4 \cdot 4H_2O$ (or fs DNA) in Tris–NaCl buffer solution of pH 7.0. Electronic absorption spectra of EB were also recorded before and after the addition of fs DNA and [Cu_2(DL-Asp)(phen)$_3$]$SO_4 \cdot 4H_2O$ in the same buffer.

Emission fluorescence spectra of [Cu_2(DL-Asp)(phen)$_3$]$SO_4 \cdot 4H_2O$ were recorded in the absence and presence of fs DNA (excitation wavelength: 520 nm). Emission fluorescence spectra of EB and system containing constant concentration of EB and fs DNA were also recorded while varying the concentration of [Cu_2(DL-Asp)(phen)$_3$]$SO_4 \cdot 4H_2O$ under the same excitation wavelength.

2.4.2. Parallel factor analysis (PARAFAC) study

The reaction solutions were prepared by adding the constant concentration of EB and fs DNA but varying concentration of [Cu_2(DL-Asp)(phen)$_3$]$SO_4 \cdot 4H_2O$ into 11(or 6) or 10 of the 11 (or 5 of the 6) 10-ml colorimetric tube, respectively. Binding reaction took place at a room temperature of 20 °C. The three-dimension (3D) fluorescence spectra were recorded after the equilibrium of complex reaction was reached. Tris–NaCl buffer of pH 7.0 was used as blank solution and subtracted. The spectra as well as concentrations of EB-DNA and EB in the equilibrious mixtures were resolved by the PARAFAC program compiled in MATLAB.

3. Results and discussion

3.1. Synthesis, characterization of the complex [Cu_2(DL-Asp)(phen)$_3$]$SO_4 \cdot 4H_2O$

3.1.1. Synthesis

[Cu_2(DL-Asp)(phen)$_3$]$SO_4 \cdot 4H_2O$ was prepared from a reaction of cupric acetate with 1,10-phenanthroline and DL-aspartic acid, with sulfuric acid adjusting the pH. The reaction took place in ethanol water solution, with the final volume ratio of 1:4. The complex was easily prepared and purified. It is very stable in air. It can be dissolved in water and methanol, and was slightly soluble in ethanol, but almost insoluble in nonpolar solvents, such as ethyl acetate, et al.

3.1.2. Infrared spectra

The infrared spectra of the complex provide significant indications for the structure of the isolated complex. The analysis of the infrared spectra [21] is as follows:

(1) The infrared spectra of the complex shows a band in the 3478–3380 cm^{-1} range, which can be assigned to the free OH-group stretching vibration.
(2) Two bands in the 3221–3078 cm^{-1} region of the complex can be assigned to NH-group stretching vibration. Compared with the NH-group in free DL-aspartic acid (3022–2830 cm^{-1}), the two bands both shift to higher wave numbers. This indicates that N atom has coordinated to the central copper atom.
(3) The band in the 2950–2880 cm^{-1} range on the infrared spectra of the complex can be assigned to the CH_2-group stretching vibration which is very weak in free DL-aspartic acid. The bending vibration of CH_2 shifts to 1300 cm^{-1}, lower wave numbers compared with the same vibration of free DL-aspartic acid at 1357 cm^{-1}. It is speculated that such changes are induced by the coordination to copper atom of β-COO^-.
(4) Compared with the COO^--group of free DL-aspartic acid ($\nu_{as} = 1614\,cm^{-1}$, $\nu_s = 1419\,cm^{-1}$), the complex displays

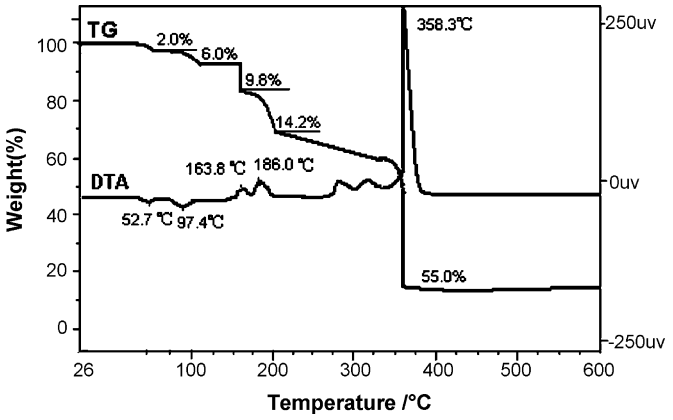

Fig. 2. TG and DTG curves of $[Cu_2(DL\text{-}Asp)\ (phen)_3]SO_4{\cdot}4H_2O$.

two bands of the symmetric stretching vibration of COO^--group at 1655 and 1575 cm^{-1}, shifting to higher and lower wave numbers, respectively; one asymmetric vibration at 1402 cm^{-1}, shifting to lower wave numbers; the $\Delta\nu$ is 243 and 173 cm^{-1}, respectively. Only one $\Delta\nu$ is larger than 200 cm^{-1}, which indicates that the monodentate coordination to copper atom is just of one COO^--group, and bidentate coordination takes place of the other one [22]. The α-COO^- is thought to be monodentate, considering the stabilization of coordination.

(5) The complex shows a band at 1521 cm^{-1}, which can be assigned to the stretching vibration of C=N; two bands at 850 and 726 cm^{-1}, which can be assigned to the bending vibration CH-group of phenanthroline. Compared with the free phenanthroline (856 and 750 cm^{-1}), they both shift to lower wave numbers, indicating that the two N atoms of phenanthroline have coordinated to the central copper atom [23].

(6) The bands at 563 and 440 cm^{-1} can be assigned to the N–M and O–M stretching vibration, which is nonexistent in the ligands [24].

(7) The complex also displays a band at 1101 cm^{-1}, which can be assigned to the stretching vibration of free SO_4^{2-}.

3.1.3. Thermal analysis

The TG and DTA curves of $[Cu_2(DL\text{-}Asp)(phen)_3]SO_4{\cdot}4H_2O$ are shown in Fig. 2. The TG curve indicates that the complex under investigation shows five main distinct steps that are maximized at 52.7, 97.4, 163.8, 186.0 and 358.3 °C on DTA curve. The first main decomposition stage indicates that, occurring at 44.5–55.0 °C, the complex suffers 2.0% weight loss that corresponds to one mole crystalline water (calculated: 1.9%). The second step indicates that, occurring at 85.8–102.5 °C, the weight lost of the complex is 6.0%, which corresponds to three other moles crystalline water (calculated: 5.6%). The third step indicates that, occurring at 156.6–172.3 °C, the weight lost is 9.8%, which corresponds to one mole SO_4^{2-} (calculated: 9.9%). The fourth step indicates that, occurring at 173.5–202.0 °C, the weight lost is 14.2%, which corresponds to one mole Asp^{2-} (calculated: 13.6%). The last step indicates that the complex suffers 55.0% weight loss at this step occurring at 276.0–376.7 °C, corresponding to three moles phenanthroline (calculated: 55.9%). There is no more weight lost above the temperature of 400 °C. The decomposition residue presented black, which is thought to be CuO.

3.2. Spectroscopic studies of the interactions with DNA

The DNA binding modes give insights into the understanding of the biochemical mechanism of action of the complexes. Recently, studies on some ternary complexes [Cu(phen)(AA)] (AA = amino acids) indicate that the size, shape, and polarity of the side chains of different amino acids in these ternary complexes may influence their binding modes to DNA [9,25].

When $[Cu_2(DL\text{-}Asp)(phen)_3]SO_4{\cdot}4H_2O$ with different concentrations were added to 4.71×10^{-5} M DNA, the changes of the electronic absorption spectra are shown in Fig. 3(a). The DNA absorption at 260 nm takes on gradual decreasing hyperchromism as well as a little red-shift (1 nm at most) in the ratio range of 0–0.25. It presents no more hyperchromism but still a little red-shift after that, except for the molar ratio of 0.35. Hyperchromism and hypochromism are the spectral features of DNA concerning of its double helix structure. Hyperchromism means the breakage of the DNA secondary structure; and hypochromism means the DNA binding mode of complex is electrostatic effect [26]. Either red-shift or blue-shift means that the complex may have some effect on DNA [27]. Therefore, it is speculated that the complex may interact with DNA by at least two modes. At low molar ratio, the end of four-coordinated Cu(II) with a smaller "weight" precedes the six-coordinated one to bind with DNA by hydrogen bond, which is formed between the $-NH_2$ group of the ligand DL-aspartic acid and the N7 or O6 sites of intrastrand guanine bases [28]. This induces the breakage of the DNA secondary structure. However, with the addition of the complex, the hydrogen bond is gradually saturated; the complex may mainly interact with DNA by a second mode that cannot be identified by this experiment.

The electronic absorption spectra of $[Cu_2(DL\text{-}Asp)(phen)_3]SO_4{\cdot}4H_2O$ in the absence and presence of fs DNA are shown in Fig. 3(b) and (c). The complex presents three bands at 204 ($\varepsilon = 3.68 \times 10^4\ M^{-1}\ cm^{-1}$), 225 ($\varepsilon = 2.92 \times 10^4\ M^{-1}\ cm^{-1}$) and 273 nm ($\varepsilon = 3.11 \times 10^4\ M^{-1}\ cm^{-1}$), which can be attributed to the $\pi \rightarrow \pi^*$ transition of the coordinated phenanthroline ligands. Seen from Fig. 3(b), when the molar ratio of DNA to complex is small (r = 0–5.0 in our studied range), all the three absorption peaks take on gradual hypochromism; the absorption peak at 204 nm gradually red-shifts to 206 nm; a new absorption peak comes into being around 294 nm. However, when the molar ratio is up to 7.8, the absorption intensity at 204, 225, 273 nm begins to come back, almost as intense as that of the complex alone; and the absorption peaks at 225 and 273 nm begin to blue-shift. Since then, with more addition of DNA, both the hyperchromism and blue-shift become more intense. When the molar ratio is 19.8, the absorption peaks at 225 and 294 nm formed at low molar ratio disappear; the one at 273 nm blue-shifts to 267 nm. Hypochromism and red-shift mean the DNA binding mode of the complex is intercalation, which involves a strong stacking interaction of the planar aromatic rings of the

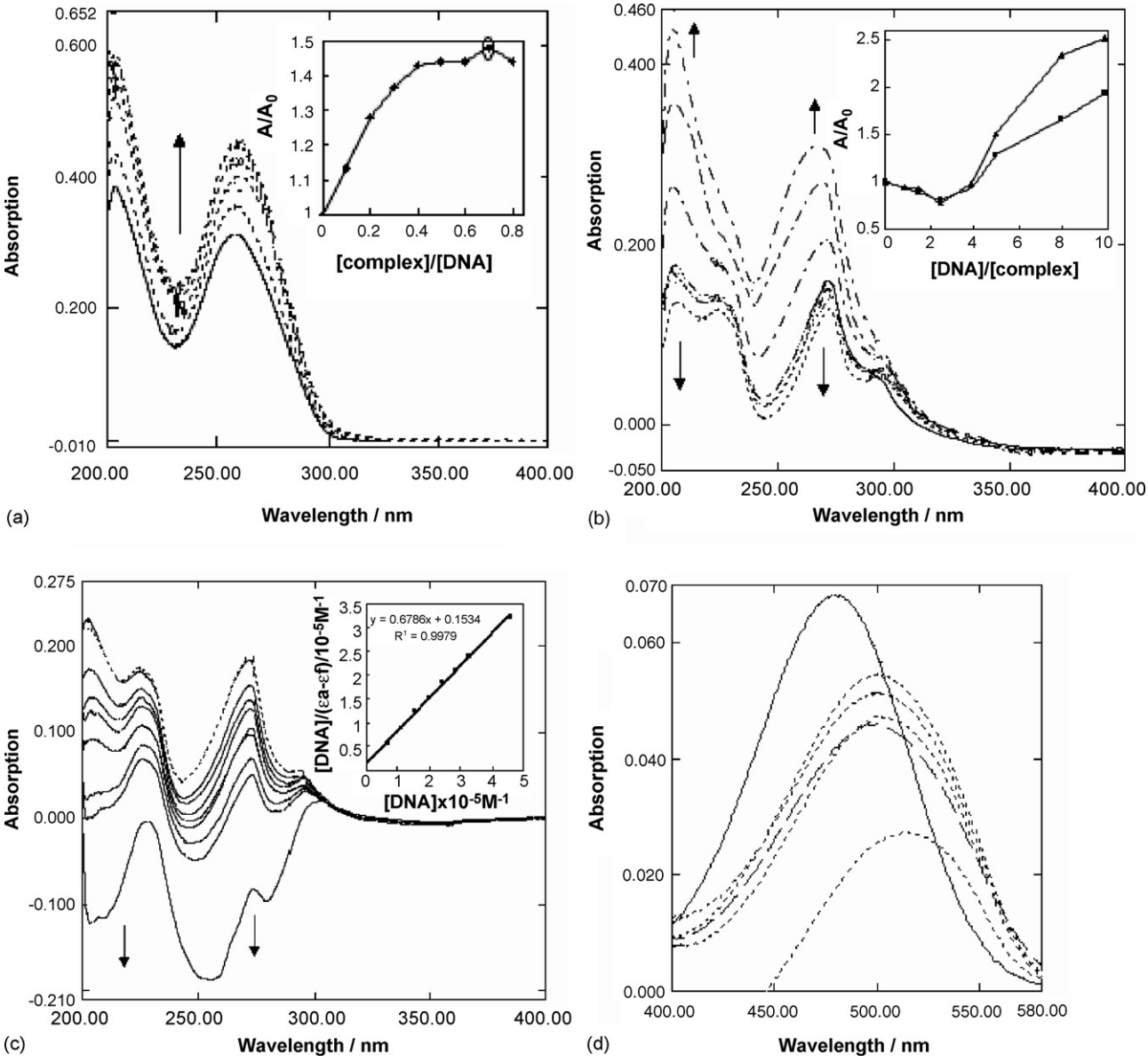

Fig. 3. Electronic absorption spectra: (a) 4.71×10^{-5} M fs DNA in the absence (—) and presence (- - -) of increasing amount of $[Cu_2(DL\text{-}Asp)(phen)_3]SO_4{\cdot}4H_2O$ at the ratio $r = 0$–0.40 with an interval of 0.05. Inset: plot A/A_0 vs. [complex]/[DNA]. (b) 5.07×10^{-6} M $[Cu_2(DL\text{-}Asp)(phen)_3]SO_4{\cdot}4H_2O$ in the absence (—) and presence of increasing amount of fs DNA: (- - -), $r = 1.8$, 3.0, 5.0; (- —), 7.8, 10.0, 15.8, 19.8. Inset: plot A/A_0 vs. [DNA]/[complex], (▲): wavelength = 273 nm, (■): wavelength = 224 nm. (c) 1.20×10^{-5} M $[Cu_2(DL\text{-}Asp)(phen)_3]SO_4{\cdot}4H_2O$ in the absence (- - -) and presence (—) of increasing amount of fs DNA at the ratio $r = 0$, 0.4, 1.8, 2.6, 3.4, 4.0, 4.8, 5.4, 7.6. Inset: plot $[DNA]/(\varepsilon_a - \varepsilon_f)$ vs. [DNA]. (d) 2.02×10^{-5} M EB in the absence (—), presence of 2.39×10^{-5} M fs DNA and $[Cu_2(DL\text{-}Asp)(phen)_3]SO_4{\cdot}4H_2O$ with different molar ratios of complex to DNA: (– –), $r = 0$; (- - -), from the top down: $r = 0.5$, 3.0, 5.0, 6.0.

coordinated ligand phenanthroline with the base pairs of DNA [2,3]. Reversely, blue-shift and hyperchromism mean another binding mode has happened, which is thought of as hydrogen bond effect by Zhang and Uma Maheswari [9,28]. In order to obtain the maximum molar ratio at which the complex interacts with DNA by intercalation and calculate the binding constant K_b, a second experiment in which the concentration of DNA was diluted has been done. The results are shown in Fig. 3(c). When the molar ratio of DNA to complex is 7.6, the shape of the spectra changes so much that the absorption peaks at 204 and 273 nm disappear or almost disappear (the hypochromicity at 273 nm is 73.1%, with red-shift of 1.2 nm), respectively; the absorption peak at 225 nm a little red-shifts to 226 nm, with hypochromicity of 60.6%; and a new absorption peak forms at 296 nm. As shown in the inset of Fig. 3(c), the $[DNA]/(\varepsilon_a - \varepsilon_f)$ is linearly correlated with [DNA], and linear relationship is significant ($R^2 = 0.9979$). The binding constant K_b of 5.2×10^6 M^{-1} was determined from the plot of $[DNA]/(\varepsilon_a - \varepsilon_f)$ versus [DNA] using the absorption at 273 nm [29]. The K_b value is even larger than EB, a classical intercalator, the K_b of which is 1.4×10^6 M^{-1} [30]). This indicates that at low molar ratio of DNA to complex (0–7.6 in our studied range), the complex has a very high binding affinity to DNA. Compared with 6.35×10^3 M^{-1}, the DNA binding constant of $[Cu(phen)(L\text{-}Thr)(H_2O)](ClO_4)$ [9], it is concluded

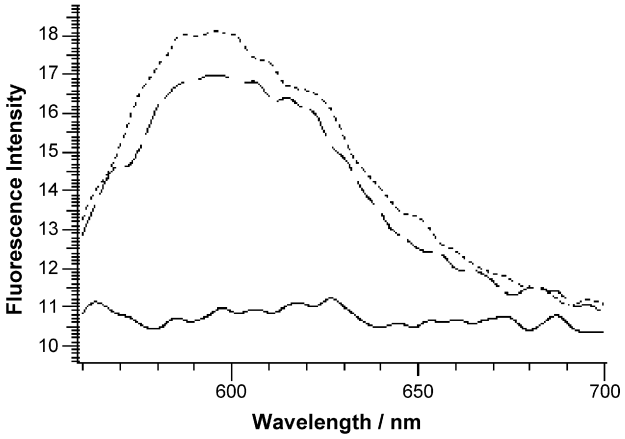

Fig. 4. Fluorescence intensity of 5.57×10^{-6} M $[Cu_2(DL\text{-}Asp)(phen)_3]SO_4{\cdot}4H_2O$ in the absence (—) and presence of different concentration of fs DNA at the molar ratio of DNA to complex: (– –), $r = 1$; (- - -), $r = 2$.

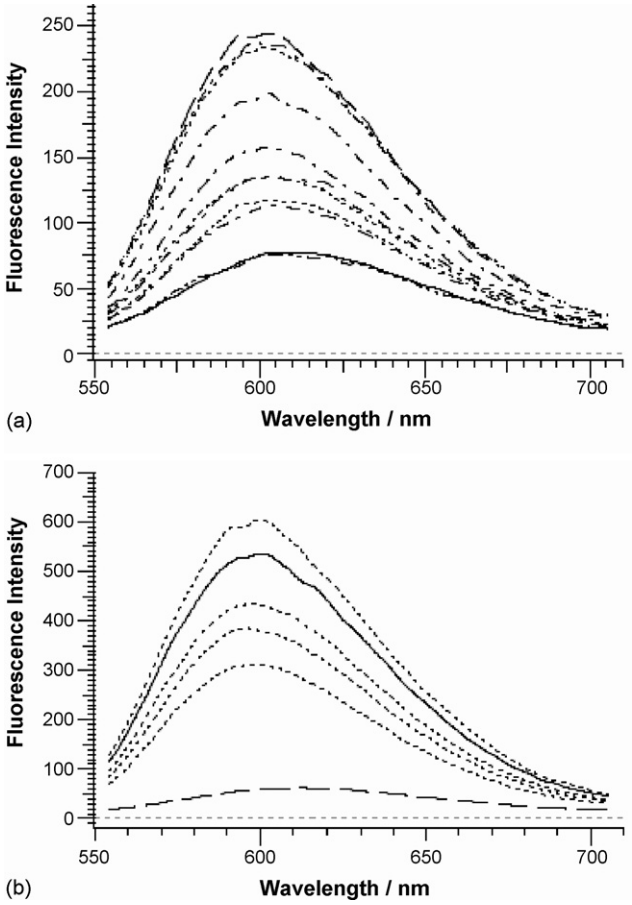

Fig. 5. (a) Fluorescence intensity of 1.52×10^{-5} M EB (—), EB-DNA ($c_{DNA} = 7.14 \times 10^{-6}$ M) (– –) and presence of $[Cu_2(DL\text{-}Asp)(phen)_3]SO_4{\cdot}4H_2O$ at different molar ratio of complex to DNA: (- —), from the top down: $r = 0.25$, 0.2, 0.15, 0.1, 0.05; (- - —), $r = 0.35$; (- —), $r = 0.3$, 0.4, 0.45. (b) Fluorescence intensity of 1.12×10^{-5} M EB (– –), EB-DNA ($C_{DNA} = 2.5 \times 10^{-5}$ M) (—) and presence of $[Cu_2(DL\text{-}Asp)(phen)_3]SO_4{\cdot}4H_2O$ at different molar ratio of the complex to DNA: (- - -), from the top down: $r = 0.5$, 3.0, 5.0, 6.0.

that the six-coordinated Cu(II) atom with two phenanthroline molecules has a much higher binding affinity to DNA than the five-coordinated one with one phenanthroline molecule. Also, it can be seen from the results of these two experiments that, when the concentration of DNA is small, intercalation is likely the main interaction with the six-coordinated Cu(II) end of the complex; other wise, the hydrogen binding takes place with the four-coordinated Cu(II) end. These results well validate the ones of Fig. 3(a).

As shown in Fig. 3(d), 2.02×10^{-5} M EB has an absorption peak at 479 nm, with the absorption intensity of 0.068. With the addition of 2.39×10^{-5} M fs DNA solution, the absorption peak red-shifts to 499 nm with the hypochromicity of 32.3%. This just accords with the fact that EB is an intercalator [31]. Compared with the spectra of EB in the presence of DNA alone, the absorption peak red-shifts to 500 nm with hyperchromicity of 23.8% at the molar ratio of complex $[Cu_2(DL\text{-}Asp)(phen)_3]SO_4{\cdot}4H_2O$ to DNA of 0.5. This indicates that the interaction between the complex and DNA is not intercalation which competes for the same site of DNA with EB [32]. When the molar ratio is 3.0–6.0, the absorption peak gradually presents stronger bathochromic effect and hypochromism (the hypochromicity is 42.8% with red-shift of 15 nm at the ratio of 6.0). This much more indicates that the complex may not compete for the same site with EB. However, these results are different from those of the anterior three figures of Fig. 3, indicating that more experiments should be carried out to make sure the interactions between the complex and DNA; or between the complex, EB and DNA.

Energy change caused by the collision between solvent and complex molecules induces fluorescence quenching. DNA, as a hydrophobic macromolecule, can prevent quenching and increase the fluorescence of the complex when binding with it, especially in the form of intercalation [33]. As shown in Fig. 4, little luminescence is observed for the aqueous solution of $[Cu_2(DL\text{-}Asp)(phen)_3]SO_4{\cdot}4H_2O$. Although the fluorescence spectra are not very smooth due to the small concentration, it can still be seen that, the fluorescence intensity gradually increased and saturated with the addition of DNA. This indicates that the complex may bind with DNA by intercalation, and supports the results of Fig. 3(a)–(c).

EB is a probe for DNA structure detection. Its fluorescence intensity is highly increased when intercalating into the base pair of DNA (when [DNA]/[EB] = 0.5 and 2.2, the fluorescence intensity is 1.7 and 8.5 times of that of EB alone, respectively). However, the enhanced fluorescence can be quenched evidently when there is a second complex that can replace the bound EB or break the secondary structure of DNA [33]. As shown in Fig. 5(a), in our studied system, when the molar ratio of complex to DNA is 0.05, the decrease of the fluorescence intensity is 53.5%. With the addition of the complex till the molar ratio of 0.25, the fluorescence intensity gradually increases. After that, it gradually decreases again, except for the ratio of 0.35, at which the fluorescence intensity is almost as low as that of EB alone. These results are consistent with those of Fig. 3(a)–(c). That is, the four-coordinated Cu(II) end of the complex has the priority in binding with DNA by hydrogen bond at a small complex concentration (r ranges from 0.05 to 0.25). This induces the breakage of the DNA secondary structure and quenches the

fluorescence intensity of EB-DNA. With the addition of the complex, the hydrogen bond is gradually saturated and intercalation between the six-coordinated Cu(II) end and DNA takes place. This quenches the fluorescence intensity in a second way. Still, at the molar ratio of 0.35, the DNA secondary structure is broken again, together with the intercalation, almost drives all the EB out of the adjacent base pairs of DNA. The fluorescence intensity does not always decrease in the ratio range of 0.1–0.5; but after decreased at 0.05, it gradually increases again. Hence, it is concluded that, because of the electrostatic effect between the complex cation and the phosphate group of DNA [26] and the conformational stabilization, the double helix structure of DNA gradually resumes; EB intercalates into the base pair again. This enhances the fluorescence intensity. In order to get full understandings of the DNA binding modes of the complex, experiments with the molar ratio of the complex to DNA ranging from 0.5 to 6.0 have also been done. The fluorescence spectra are shown in Fig. 5(b). With the addition of the complex, the fluorescence intensity is gradually quenched, except for the ratio of 0.5, at which the fluorescence intensity is even higher than that of EB-DNA. Just as the analysis of Fig. 3(c), it is still concluded that, the six-coordinated Cu(II) end of the complex mainly binds with DNA by intercalation in this molar ratio range. For the ratio of 0.5, it is still thought of as electrostatic effect, which can stabilize the double helix and induce the intercalation of more EB molecules into the adjacent base pair of DNA. Still, the results do not accord with those of Fig. 3(d), but well conform to those of Figs. 3(b), (c) and 4.

By the analysis of all the results above, it is known that full understanding of the DNA binding modes cannot be obtained just by two-dimensional spectroscopic methods.

Table 1
The core consistency and explained variance of EB-DNA system at the molar ratio range of $[Cu_2(DL\text{-}Asp)(phen)_3]SO_4{\cdot}4H_2O$ to DNA (r = 0–0.45) using different number of components

Number of components	1	2	3	4	5	6
Core consistency (%)	100	100	88.19	39.41	16.73	1.69
Explained variance (%)	96.68	98.08	98.14	98.17	98.17	98.19

3.3. PARAFAC studies of the interactions with DNA

With the development of chemometric algorithm for high order data, in particular for the trilinear excitation-emission fluorescence data array, it becomes possible to study the interactions of metal complexes with DNA by PARAFAC algorithm. From this method, one can directly obtain the DNA binding modes without utilizing Scatchard plot [30], as well as the equilibrium concentrations of all fluorescing chemicals with a proper intensity.

In this paper, the appropriate number of components is determined based on several criteria—the visual appearance of loadings, the variance explained by the model and the core consistency (a so-called Tucker3-like core array is calculated from the data and the PARAFAC loadings. The relative sum-of-squared difference between this core and a superdiagonal core of ones is called the core consistency. It is usually expressed as a percentage). It provides a quantitative measure of how well the loadings represent variation in the date consistent with this assumption [34].

As shown in Tables 1 and 2, compared the increase of the explained variance and the decrease of the core consistency, it is known that for the two mixture series, the best number of

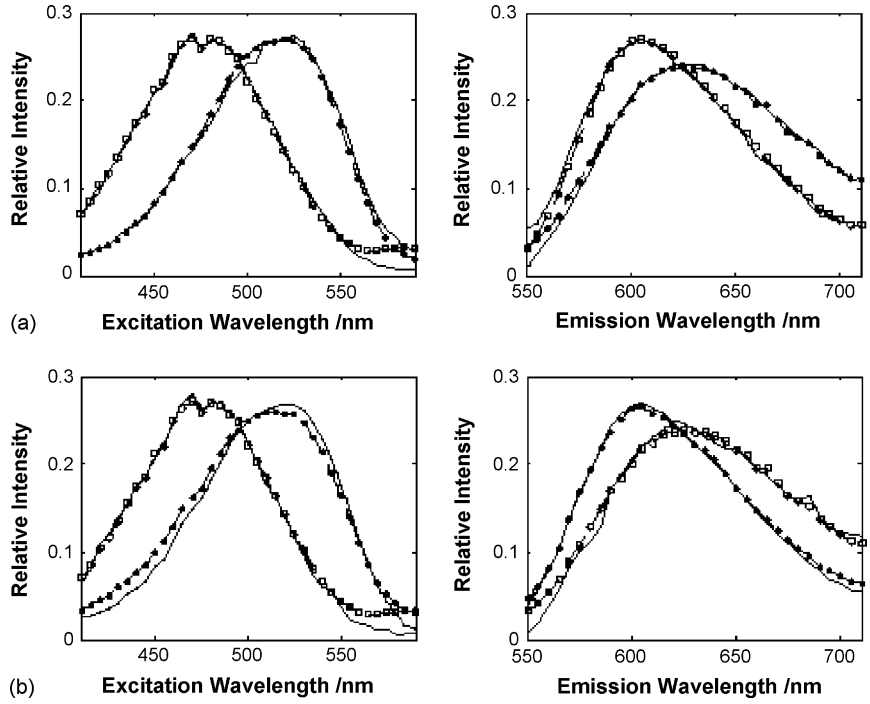

Fig. 6. Excitation (left) and emission (right) fluorescence spectra at different molar ratio range of the complex to DNA (a) 0–0.45; (b) 0, 0.5–6.0, resolved by PARAFAC using three components, solid and dashed lines are the resolved and recorded spectra, respectively, of EB-DNA (●) and EB (◯).

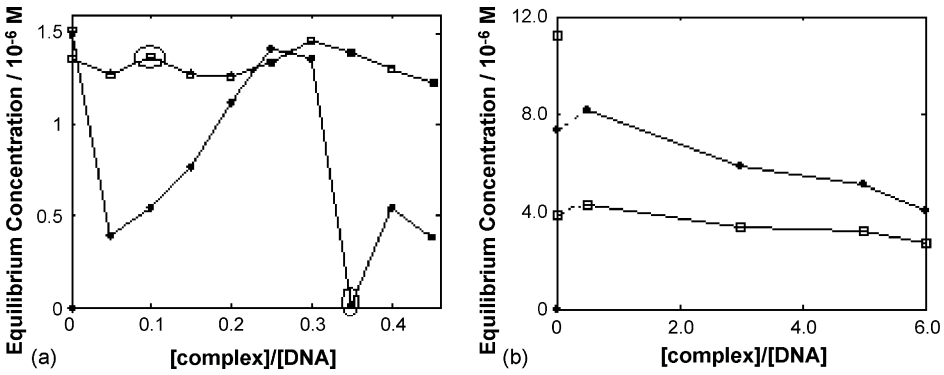

Fig. 7. Equilibrium concentrations of EB-DNA (●) and EB (◯) calculated using three components, at different molar ratio ranges of the complex to DNA: (a) of 0–0.45 (the concentration of EB-DNA is 10 times enlarged); (b) 0, 0.5–6.0.

components are both three [34]. The excitation and emission spectra of EB-DNA and EB resolved by PARAFAC algorithm using component three are shown in Fig. 6. It can be seen that the resolved spectra match the recorded ones well. The concordance of the resolved two spectral profiles corresponding to the first two components with the excitation and emission spectra of EB-DNA and EB, confirms that the resolved concentration values corresponding to these two components are concentrations of EB-DNA and EB in corresponding reaction mixtures. Both the equilibrium concentration profiles of EB-DNA and EB of the two mixture series are shown in Fig. 7.

The mixture series of 11 samples containing same initial amount of EB and DNA but increased initial concentration of $[Cu_2(DL\text{-}Asp)(phen)_3]SO_4{\cdot}4H_2O$ was studied. The equilibrium concentrations of EB-DNA and free EB are shown in Fig. 7(a). With the addition of DNA, the concentration of EB-DNA increases and that of free EB decreases, indicating that some EB has intercalated into the DNA base pair. When $[Cu_2(DL\text{-}Asp)(phen)_3]SO_4{\cdot}4H_2O$ is added with the molar ratio to DNA of 0.05, both the concentrations of EB-DNA and EB decrease. After that, when the molar ratio ranges from 0.1 to 0.25, both the concentrations of EB-DNA and EB gradually increase, except for the ratio of 0.1, at which a "disturbance" happens to EB. It is still concluded that, in the molar ratio range of 0.05–0.25, the complex binds with DNA by hydrogen bond that is gradually saturated, inducing the breakage of the DNA secondary structure. However, as a result of the electrostatic effect between the complex cation and the phosphate group as well as the conformational stabilization of DNA, it can gradually resume the primary double helix structure. EB intercalates into the DNA base pair again, increasing the concentration of EB-DNA. If EB interacted with DNA only by intercalation, the concentration of free EB would increase with the breakage of the DNA secondary structure at the molar ratio of 0.05. On the contrary, the concentration of EB decreases (Fig. 7(a)). Therefore, it is concluded that, the conformation of DNA changes from B form to BZ mixed form with the addition of the complex; and EB may interact with DNA by cooperative binding, another binding mode besides intercalation [20,35]. Consequently, the concentration of free EB decreases. When the molar ratio ranges from 0.5 to 1.5, the BZ-DNA starts to resume to B-DNA, inducing the instability of DNA conformation and resulting in the "disturbance" of free EB concentration. After that, with the comeback of the B-DNA conformation, more intercalation takes place while the cooperative binding is gradually destroyed, releasing more and more free EB. When the molar ratio ranges from 0.3 to 0.45, the concentration of EB-DNA gradually decreased, except for the ratio of 0.35, at which the concentration of EB-DNA is extremely small; and for free EB, after up to the maximum concentration at the ratio of 0.3, it also gradually decreases. Consequently, in this molar ratio range, the six-coordinated Cu(II) end of the complex interacts with DNA by intercalation, which drives EB out of the DNA base pair. Correspondingly, the four-coordinated Cu(II) end interacts with DNA by hydrogen bond existing in the major and minor grooves of DNA [9,14]. This changes the DNA conformation from B form to the BZ mixed form. Again, EB interacts with BZ-DNA by cooperative binding, which decrease the concentration of free EB. At the molar ratio of 0.35, the breakage of the secondary structure of DNA takes place again, together with intercalation between the complex and DNA, decreases the concentration of EB-DNA. Due to the low fluorescence intensity, no $[Cu_2(DL\text{-}Asp)(phen)_3]SO_4{\cdot}4H_2O$ or compound formed by the complex binding with DNA in the form of intercalation is found. The results above conform well to the results of Figs. 3(a), (b), (c), 4 and 5(a).

Table 2
The core consistency and explained variance of EB-DNA system at the molar ratio of $[Cu_2(DL\text{-}Asp)(phen)_3]SO_4{\cdot}4H_2O$ to DNA ($r = 0, 0.5–6.0$) using different number of components

Number of components	1	2	3	4	5	6
Core consistency (%)	100	100	96.33	47.71	9.67	2.68
Explained variance (%)	98.26	99.06	99.16	99.35	99.36	88.23

The other mixture series of six samples containing same initial amount of EB and DNA and increased initial concentration of $[Cu_2(DL\text{-}Asp)(phen)_3]SO_4{\cdot}4H_2O$ was also studied. The equilibrium concentrations of EB-DNA and free EB are shown in Fig. 6(b). Still, with the addition of DNA, the intercalation of EB to DNA is indicated by the increase of EB-DNA and the decrease of free EB. At the molar ratio of 0.5, concentration increase hap-

pens to both EB-DNA and EB for electrostatic effect, which can stabilize the conformation of B-DNA. Just like the molar ratio range of 0.3–0.45, both the concentrations of EB-DNA and free EB take on gradual decrease in the range of 0.5–6.0. Still, in this molar ratio range, the six-coordinated Cu(II) end of the complex interacts with DNA by intercalation, driving EB out of the DNA base pair. Correspondingly, the four-coordinated Cu(II) end interacts with DNA by hydrogen bond existing in the major and minor grooves of DNA. This changes DNA conformation from B form to the BZ mixed form. EB gradually interacts with BZ-DNA by cooperative binding, decreasing the concentration of free EB. These results not only conform well to those of Figs. 3(b), (c), (d) and 5(b), but also explain why the absorption spectra of EB take on such changes with the addition of $[Cu_2(DL\text{-}Asp)(phen)_3]SO_4{\cdot}4H_2O$ in Fig. 3(d). Likewise, the results of PARAFAC indicate that with more addition of the complex, the BZ-DNA would have more intense trend to form. This DNA conformation has a higher affinity to EB by cooperative binding than the B-DNA binding with EB by intercalation. This exactly accords with Suh [35], who got the same conclusion by circular dichroic spectra, analyzed by singular value decomposition.

4. Conclusion

This paper reports a new kind of copper(II) complex $[Cu_2(DL\text{-}Asp)(phen)_3]SO_4{\cdot}4H_2O$; and characterizes it by element analysis, infrared spectra, and thermal analysis. The complex is easy to synthesize, and has good air-stability and water-solubility. The fs DNA binding modes of the complex were studied by using electronic absorption spectra, fluorescence spectra and PARAFAC algorithm. All spectroscopic studies except one with an unaccustomed change of EB, indicate that when the molar ratio of complex to DNA is smaller than 0.25, the four-coordinated Cu(II) end of the complex mainly binds with DNA by hydrogen bond. This breaks the secondary structure of DNA. Otherwise, the six-coordinated Cu(II) end of the complex mainly interacts with DNA by intercalation. Besides these two interactions, electrostatic effect also takes place. The equilibrium concentrations of EB-DNA and EB can be directly obtained from the PARAFAC algorithm. The corresponding results not only well conform to those of the spectroscopic studies, but also explain the one which has different results from others. That is, by the interaction with the complex, the fs DNA conformation is changed from B form to BZ mixed form. The latter may interact with EB by cooperative binding, which has a higher affinity than intercalation. They strongly support our conjecture of the DNA binding modes of the complex. The PARAFAC algorithm is proved a convincing method in studying the DNA binding modes of complexes.

Acknowledgement

This work was supported by the National Natural Science Foundation of China (No. 20371043).

References

[1] M.C. Linder, Mut. Res. 475 (2001) 141–152.
[2] D.S. Sigman, D.M. Perrin, Chem. Rev. 93 (1993) 2295–2316.
[3] F. Schaeffer, S. Rimsky, A. Spassky, J. Mol. Biol. 260 (1996) 523–539.
[4] S. Mahadevan, M. Palaniandavar, Inorg. Chem. 37 (1998) 3927–3934.
[5] A. Bouskila, B. Drahi, E. Amouyal, I. Sasaki, A. Gaudemer, J. Photochem. Photobiol. A: Chem. 163 (2004) 381–388.
[6] J.D. Ranford, P.J. Sadler, Dalton. Trans. (1993) 3393–3399.
[7] M. Geraghty, V. Sheridan, M. McCanna, M. Devereuxb, V. McKeec, Polyhedron 18 (1999) 2931–2939.
[8] D.K. Saha, U. Sandbhor, K. Shirisha, S. Padhye, D. Deobagkar, C.E. Ansond, A.K. Powelld, Bioorg. Med. Chem. Lett. 14 (2004) 3027–3032.
[9] S.-C. Zhang, Y.-G. Zhu, C. Tu, H.-Y. Wei, Z. Yang, L.-P. Lin, J. Ding, J.-F. Zhang, Z.-J. Guo, J. Inorg. Biochem. 98 (2004) 2099–2106.
[10] K.E. Erkkila, D.T. Odom, J.K. Barton, Chem. Rev. 99 (1999) 2777–2796.
[11] D.S. Sigman, Biochemistry 29 (1990) 9097–9105.
[12] D.S. Sigman, A. Mazumder, D.M. Perrin, Chem. Rev. 93 (1993) 2295–2316.
[13] W.K. Pogozelski, T.D. Tullius, Chem. Rev. 98 (1998) 1089–1108.
[14] R. Ren, P. Yang, W. Zheng, Z. Hua, Inorg. Chem. 39 (2000) 5454–5463.
[15] H.-P. Xie, X. Chu, J.-H. Jiang, H. Cui, G.-L. Shen, R.-Q. Yu, Spectrochim. Acta Part A 59 (2003) 743–749.
[16] R. Bro, Chemom. Intell. Lab. Syst. 38 (1997) 149–171.
[17] C.M. Andersen, R. Bro, J. Chemometr. 7 (2003) 200–215.
[18] J. Marmur, J. Mol. Biol. 3 (1961) 208–218.
[19] M.E. Reichmann, S.A. Rice, C.A. Thomas, P. Doty, J. Am. Chem. Soc. 76 (1954) 3047–3055.
[20] S.A. Winkle, L.S. Rosenberg, T.R. Krugh, Nucleic Acid Res. 10 (1982) 8211–8222.
[21] K. Nakamoto, Infrared and Raman Spectra of Inorganic and Coordination Compounds, 3rd ed., Wiley, New York, 1978.
[22] S.D. Robinson, M.F. Uttley, J. Chem. Soc. Dalton Trans. (1973) 1912–1920.
[23] W.-L. Shi, D.-Y. Chen, Q.-Z. Wu, Spectroscopy Spectral Anal. 3 (2004) 327–329 (in Chinese).
[24] A.M. Ramadan, J. Inorg. Biochem. 65 (1997) 183–189.
[25] M. Chikira, Y. Tomizawa, D. Fukita, T. Sugizaki, N. Sugawara, T. Yamazaki, A. Sasano, H. Shido, M. Palaniandavar, W.E. Antholine, J. Inorg. Biochem. 89 (2002) 163–173.
[26] P. Yang, M.-L. Guo, B.-S. Yang, Chinese Sci. Bull. 39 (1994) 997–1002.
[27] Z.-G. Zhang, P. Yang, M.-L. Guo, H.-F. Wang, J. Inorg. Biochem. 63 (1996) 183–190.
[28] P. Uma Maheswari, M. Palaniandavar, J. Inorg. Biochem. 98 (2004) 219–230.
[29] A. Wolf, G.H. Shimer, T. Meehan, Biochemistry 26 (1987) 6392–6396.
[30] J.B. Lepecq, C. Paoletti, J. Mol. Biol. 27 (1967) 87.
[31] E.C. Long, J.K. Barton, Acc. Chem. Res. 23 (1990) 273–276.
[32] C.G. Reinhardt, T.R. Krugh, Biochemistry 17 (1978) 4845–4854.
[33] Y.-F. Song, P. Yang, Polyhedron 20 (2001) 501–506.
[34] R. Bro, H.A.L. Kiers, J. Chemometr. 17 (2003) 274–286.
[35] D. Suh, Exp. Mol. Med. 31 (1999) 151–158.